

# **Biom mineralization of ferrimagnetic greigite ( $\text{Fe}_3\text{S}_4$ ) and iron pyrite ( $\text{FeS}_2$ ) in a magnetotactic bacterium**

**Stephen Mann<sup>\*</sup>, Nicholas H. C. Sparks<sup>\*</sup>,  
Richard B. Frankel<sup>†</sup>, Dennis A. Bazylinski<sup>‡§</sup>  
& Holger W. Jannasch<sup>‡</sup>**

<sup>\*</sup> School of Chemistry, University of Bath, Claverton Down,  
Bath BA2 7AY, UK

<sup>†</sup> Department of Physics, California Polytechnic State University,  
San Luis Obispo, California 93407, USA

<sup>‡</sup> Department of Biology, Woods Hole Oceanographic Institution,  
Woods Hole, Massachusetts 02543, USA

---

**THE ability of magnetotactic bacteria to orientate and navigate along geomagnetic field lines is due to the controlled intracellular deposition of the iron oxide mineral, magnetite ( $\text{Fe}_3\text{O}_4$ )<sup>1,2</sup>. The function and crystal chemical specificity of this mineral has been considered to be unique amongst the prokaryotes<sup>3</sup>. Moreover, the bacterial production of magnetite may represent a significant contribution to the natural remanent magnetism of sediments<sup>4,5</sup>. Here we report, the intracellular biom mineralization of single crystals of the ferrimagnetic iron sulphide, greigite ( $\text{Fe}_3\text{S}_4$ ), in a multicellular magnetotactic bacterium common in brackish, sulphide-rich water and sediment. We show that these crystals are often aligned in chains and associated with single crystals of the non-magnetic mineral, iron pyrite ( $\text{FeS}_2$ ). Our results have important implications for understanding biom mineralization processes and magnetotaxis in micro-organisms inhabiting sulphidic environments. Furthermore, the biogenic production of magnetic iron**

---

<sup>§</sup> Present address: Department of Anaerobic Microbiology, Virginia Polytechnic Institute and State University, Blacksburg, Virginia 24061, USA.

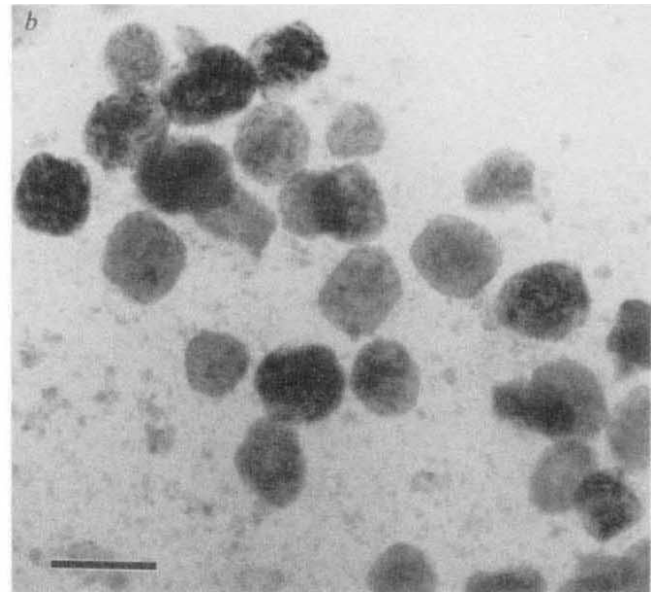
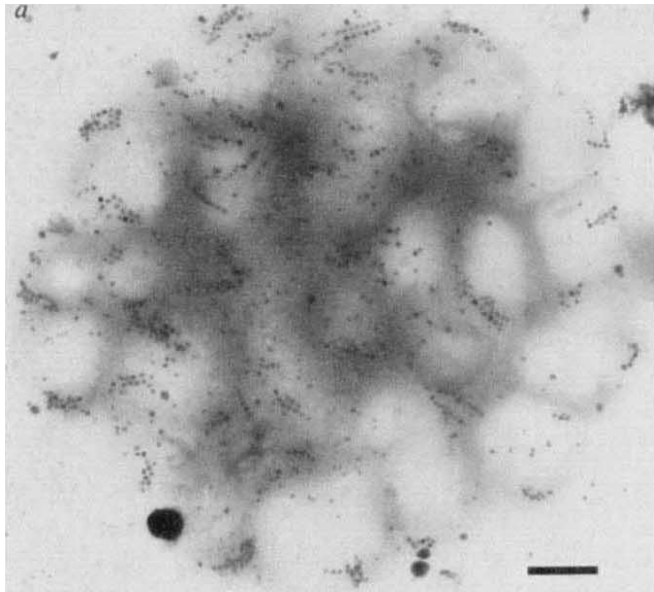


FIG. 1. *a*, Transmission electron micrograph showing a multicellular, magnetotactic bacterium containing discrete, organized, intracellular iron sulphide particles. Scale bar, 1  $\mu\text{m}$ . *b*, High-magnification image showing biomineral

particles. Note the well-defined edges of many of the particles and the non-uniform diffraction contrast indicating extensive surface roughness. Scale bar, 100 nm.

**sulphides should be considered as a possible source of remanent magnetization in sediments.**

Magnetotactic bacteria were collected from jars filled with sediment and water from several marine and brackish (12–31 p.p.t. salt) sites with high sulphide (1–2 mM). After the sediment had settled, substantial numbers of magnetotactic bacteria were collected by allowing them to accumulate at the south pole of a bar magnet placed outside the jar just above the sediment-water interface, and subsequently drawing them up with a Pasteur pipette. The predominant organism collected this way was a motile, spherical (3–8  $\mu\text{m}$  diameter) multicellular aggregate of about 7–20 individual prokaryotic cells. Each cell was roughly ovoid and bore numerous flagella on one side<sup>6</sup>. Intact organisms eventually disaggregated into a loose clump of individual cells.

Disaggregated cells retained a permanent magnetic dipole moment as evidenced by their response to reversals of the local magnetic field direction, but were non-motile. Intact organisms were deposited in water drops on carbon-coated electron microscope grids where they partially disaggregated as the drops dried. The samples were neither fixed nor stained; nickel grids were used because the sulphide-rich salt water and sediment reacted with copper grids. Particles were studied *in situ* with disaggregated cells by scanning transmission electron microscopy (STEM), high resolution transmission electron microscopy (HRTEM), electron diffraction and energy dispersive X-ray analysis (EDXA). Electron diffraction patterns were calibrated using standard materials. Data were recorded from groups of crystals and individual particles.

Figure 1*a* shows a low-magnification image of a typical disaggregated organism. Individual cells contained chains of discrete intracellular electron dense inclusions (Fig. 1*b*). On average, each chain contained 10 particles with a mean size of 75 nm. Compositional analysis showed that the particles contained Fe and S, but not O (Fig. 2). Occasionally, low levels of oxygen were detected at the edges of the particles but this was attributed to surficial oxidation of samples stored in air. These observations are similar to those of Farina *et al.*<sup>7,8</sup>, who previously studied a morphologically similar magnetotactic multicellular organism containing Fe/S-rich inclusions from marine lakes in Rio de Janeiro.

Many of the particles appeared irregular in shape, but they exhibited strong diffraction contrast (Fig. 1*b*), indicating that they were crystalline. Other particles showed rhombohedral and hexagonal outlines when viewed in projection (Fig. 1*b*). These

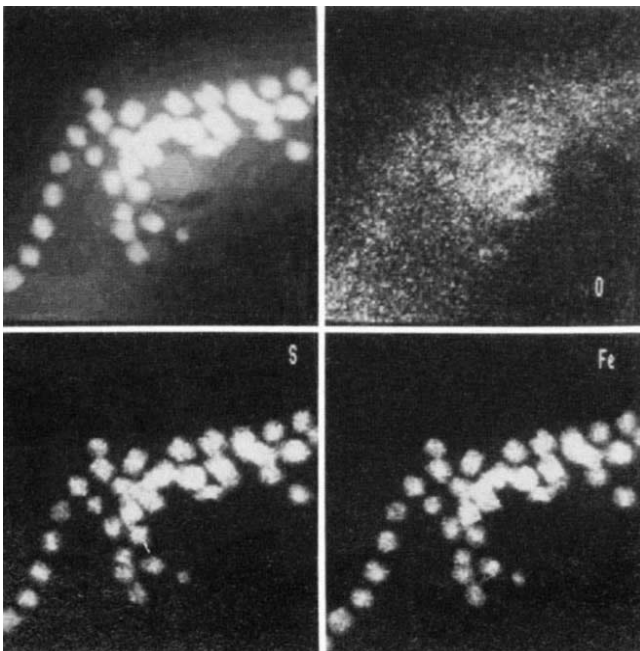


FIG. 2. Fe, S and O elemental density maps for the particles shown in the electron micrograph in the upper left part of the figure. The particles were analysed *in situ* in a magnetotactic, multicellular bacterium collected at Plum Island, Massachusetts. The maps were made by recording the respective K X-ray intensities with the energy dispersive X-ray detector at each position as the electron beam was slowly rastered across the sample. Fe and S density clearly correlate with particle position; O does not. The increased O density just below the particles correlates with increased P density (not shown), indicative of a polyphosphate granule.

images are characteristic of octahedral and cubo-octahedral particles, respectively, and indicate that the crystals could have cubic symmetry. We confirmed this by electron diffraction analysis (table 1). Powder patterns were consistent with a mixture of iron pyrite and greigite. Most of the powder patterns, however, gave  $d$  spacings corresponding to pyrite, suggesting that the magnetic mineral greigite was a minor component of the intracellular crystals. Moreover, as many of the  $d$  spacings of pyrite and greigite overlap, single-crystal diffraction patterns were required to provide unequivocal identification of the magnetic phase.

Figure 3 is a single-crystal pattern recorded from the crystal shown in the inset. The  $d$  spacings and interplanar angles (see legend for details) of this and other patterns confirmed the presence of single crystals of biogenic greigite in this organism. Other patterns corresponding to single crystals of  $\text{FeS}_2$  were also obtained. As single-crystal diffraction patterns do not rule out the presence of amorphous domains within individual crystals, lattice imaging was undertaken. But although the crystals were in general stable under the electron beam, they were too thick for successful imaging of lattice spacings. The few lattice images recorded showed that the crystals were crystallographic single-domain particles.

The identification of intracellular, discrete, organized crystals of greigite and pyrite in magnetotactic bacteria has several important implications. It is the first conclusive evidence that prokaryotes can control the mineralization of iron sulphides. Other reports on bacterial iron sulphides<sup>9-11</sup> are concerned with anaerobic biologically mediated processes, in which sulphate-reducing bacteria generate high concentrations of  $\text{H}_2\text{S}$  which subsequently combine with iron in the extracellular environment. Minerals such as pyrite, hydrotroilite, greigite and mackinawite can be deposited. In this regard, sulphate-reducing bacteria<sup>11</sup>, which can precipitate a fine-grained magnetic iron sulphide, are analogous in biomineralization terms to the anaerobic, non-magnetotactic, magnetite-producing bacterium, GS-15 (ref. 12). By contrast, the organism described here has many of the general features of biomineralization associated with genetically controlled processes. Because the environment in which it is found contains high sulphide concentrations, the organism is probably anaerobic. It is interesting that a mag-

TABLE 1 Electron diffraction data and identification of bacterial Fe sulphide inclusions

Data*	Source†	Assignment‡	
		greigite	pyrite
3.57	S	3.50 (220)	
3.16	R		3.128 (111)
3.06	S	2.98 (311)	
2.69	R		2.709 (200)
2.51	R	2.470 (400)	
2.28	S	2.26 (331)	
2.12	R		2.211 (211)
2.04	S	2.017 (422)	
1.89	R	1.901 (333)	1.915 (220)
1.71	R	1.746 (440)	
1.65	S	1.671 (531)	
1.60	R		1.633 (311)
1.55	S		1.564 (222)
1.35	R	1.383 (711)	1.354 (400)
1.26	S	1.286 (731)	
1.22	R	1.235 (800)	1.211 (420)
1.07	R	1.054 (664)	1.043 (333)
0.89	S		0.903 (600)

\* Experimental  $d$  spacings in Å.

† R, powder ring pattern; S, single crystal pattern.

‡ Standard mineral  $d$  spacings in Å. X-ray powder diffraction file: greigite (16-713), and pyrite (6-710); (hkl), Miller indices.

netotactic bacterium that produces magnetite anaerobically has been isolated from the same environment<sup>13</sup>.

There are marked similarities between the biomineralization strategies adopted for greigite and magnetite synthesis in magnetotactic bacteria. Both systems involve the formation of discrete single crystals of restricted size that are organized within the cell. We propose that the greigite crystals, like their oxide counterparts, are enclosed within an organic membrane. Indeed, some of the crystals, when imaged at high magnification, were surrounded by an amorphous sheath, but it is possible that this arises from local contamination in the electron microscope. A major difference between the bacterial greigite and magnetite crystals is that the former have a diversity of (cubic-derived)

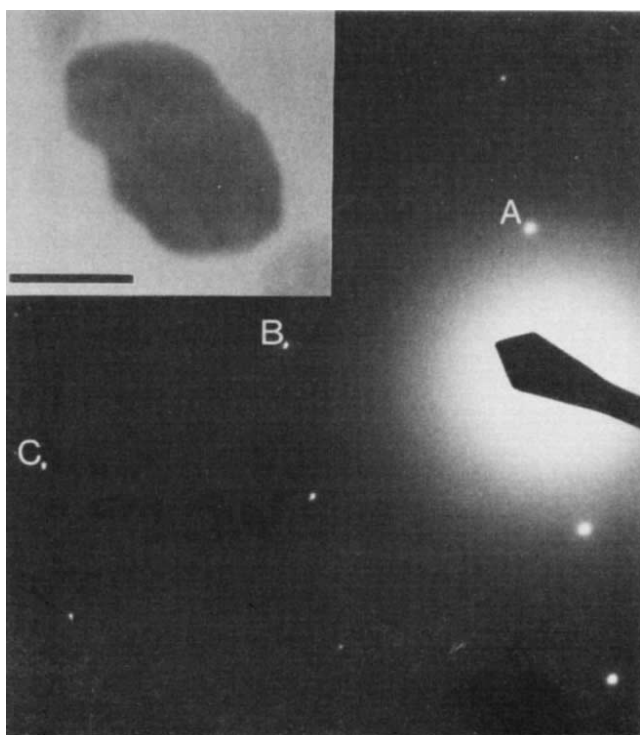


FIG. 3 Single-crystal electron diffraction pattern recorded from the crystal shown in the inset. Camera length, 284 cm;  $\lambda = 0.0251$  Å; scale bar in inset, 50 nm. The pattern corresponds to the  $[11\bar{3}]$  zone of greigite,  $\text{Fe}_3\text{S}_4$ . Reflection A,  $(2\bar{2}0)$  (3.50 Å); reflection B,  $(4\bar{2}2)$  (2.02 Å); reflection C,  $(6\bar{6}4)$  (1.054 Å). Angles:  $2\bar{2}0 \wedge 4\bar{2}2 = 73^\circ$ ,  $2\bar{2}0 \wedge 6\bar{6}4 = 90^\circ$ . Crystallographic data: space group, Fd3m (cubic);  $a = 9.876$  Å.



shapes in any one chain, whereas the latter adopt morphologies that can be unique and species-specific<sup>14</sup>. The general similarities between the two systems, however, suggests that the biological control mechanisms have much in common.

The biomineralization of bacterial magnetite involves the formation of a transient hydrous Fe(III) oxide precursor, which subsequently transforms to magnetite<sup>15,16</sup>. The presence of both greigite and iron pyrite in the organism we describe indicates that there could be a similar relationship between the two mineral phases. But under thermodynamic conditions, in a highly reducing environment at neutral pH, greigite would slowly transform to pyrite<sup>17</sup>. This implies that unless the organism continues to maintain its capacity to synthesize greigite, it would slowly lose its magnetotactic response. Thus greigite may be a metastable phase in the transformation of an undetected precursor into pyrite. Alternatively, the cells might separately mineralize greigite and pyrite by local control of iron and sulphide concentration, reducing potential and pH.

Structurally, Fe<sub>3</sub>S<sub>4</sub> and Fe<sub>3</sub>O<sub>4</sub> are isomorphous, both materials adopting the face-centred cubic spinel structure. Whether this structural similarity has relevance to the cellular mechanisms of their synthesis is unclear. In terms of their magnetic properties, the saturation magnetization of greigite is about one-third that of magnetite<sup>18</sup>. The permanent magnetic single-domain size range for greigite has not been determined but is probably similar to magnetite, because the magnetic ordering temperatures and magnetic anisotropy constants of the two minerals are similar<sup>18</sup>. Thus, the 75-nm biogenic greigite particles are likely to be permanent magnetic single domains and responsible for the magnetotactic response of the intact organism. Organization of these particles into chains would result in a parallel alignment of the individual particle moments along the chain direction, and would give each constituent cell a permanent magnetic dipole moment equal to the sum of the individual particle moments in the chain. The net magnetic dipole moment of the intact organism would then be the vector sum of the moments of the constituent cells.

Finally, we note that greigite has been identified as a source of remanent magnetism in sediments<sup>19</sup>. These deposits may be of inorganic origin, biologically mediated by sulphate-reducing micro-organisms or resulting from the diagenesis of bacterial magnetite<sup>19,20</sup>. We note, however, that the crystal size and shape of sediment greigite is similar to that reported here for bacterial greigite, and therefore propose that biogenic minerals should be considered as a further possible source of remanent magnetism in sulphide-rich sediments. □

Received 18 September; accepted 1 November 1989.

1. Frankel, R. B., Blakemore, R. P. & Wolfe R. S. *Science* **203**, 1355-1356 (1979).
2. Blakemore, R. P. A. *Rev. Microbiol.* **36**, 217-238 (1982).
3. Lowenstam, H. A. & Weiner, S. *On Biomineralization* (Oxford University Press, 1989).
4. Peterson, N., von Döbeneck, T. & Vali, H. *Nature* **320**, 611-615 (1986).
5. Stolz, J. F., Chang, S.-B. R. & Kirschvink, J. L. *Nature* **321**, 849-851 (1986).
6. Blakemore, R. P., Blakemore, N. A., Bazylinski, D. A. & Moench, T. T. *Bergey's Manual of Systematic Bacteriology* Vol. 3 (eds Staley, J. T. et al.) 1882-1889 (Williams and Wilkins, Baltimore, 1989).
7. Farina, M., Lins de Barros, H. G. P., Esquivel, D. M. S. & Danon, J. *Biol. Cell.* **48**, 85-86 (1983).
8. Farina, M., Sollarazano, G. & Viera, G. J. *Proc. Xlth Int. Cong. on Electron Microscopy (Kyoto)* 3369-3370 (1986).
9. Hallberg, R. O. *Stockholm Contr. Geol.* **13**, 35-37 (1965).
10. Hallberg, R. O. N. *Jahrbuch Mineral. Monatshefte* 481-500 (1972).
11. Freke, M. & Tate, D. J. *Biochem. microbiol. technol. Eng.* **3**, 29-39 (1961).
12. Lovely, D. R., Stolz, J. F., Nord, G. L. Jr & Phillips, J. P. *Nature* **330**, 252-254 (1987).
13. Bazylinski, D. A., Frankel, R. B. & Jannasch, H. W. *Nature* **334**, 518-519 (1988).
14. Mann, S. & Frankel, R. B. in *Biomineralization: Chemical and Biochemical Perspectives* (eds Mann, S., Webb, J. & Williams, R. J. P.) 389-426 (VCH, Weinheim, 1989).
15. Frankel, R. B., Papafthymiou, G. C., Blakemore, R. P. & O'Brien, W. D. *Biochim. biophys. Acta* **763**, 147-159 (1983).
16. Mann, S., Frankel, R. B. & Blakemore, R. P. *Nature* **310**, 405-407 (1984).
17. Berner, R. A. *Am. J. Sci.* **265**, 773-785 (1967).
18. Spender, M. R., Coey, J. M. D. & Morrish, A. H. *Can. J. Phys.* **50**, 2313-2326 (1972).
19. Demitrack, A. in *Magnetite Biomineralization and Magnetoreception in Organisms* (eds Kirschvink, J. L., Jones, D. D. & MacFadden, B. J.) 625-645 (Plenum New York, 1985).
20. Morse, J. W., Millero, F. J., Cornwell, J. C. & Rickard, D. *Earth Sci. Revs* **24**, 1-42 (1987).

ACKNOWLEDGEMENTS. We thank A. Garratt-Reed for assistance with the STEM measurements and R. P. Blakemore, F. G. Rogers, H. Lins de Barros and D. Esquivel for discussions. S.M. and N.H.C.S. were supported by the UK Science and Engineering Research Council. R.B.F. was supported by the US National Science Foundation. D.A.B. and H.W.J. were supported by the US National Science Foundation and the Office of Naval Research.